JOURNAL OF COMPUTATIONAL PHYSICS 7, 327–345 (1971)

On Finding the Admittance Matrix of a Thin-Film Network by Solving the Reduced Wave Equation in Two Dimensions

JAMES L. BLUE

Bell Telephone Laboratories, Incorporated, Murray Hill, New Jersey

Received September 10, 1970

An economical method is presented for numerically finding the admittance matrix, at any frequency, of a thin-film distributed resistance-capacitance network. The partial differential equation for the potential in the thin film,

$$\nabla^2\varphi = \gamma^2\varphi,$$
$$\gamma^2 = i\omega R_s C,$$

is reformulated as an integral equation over the boundary of the film and solved by collocation. For a given accuracy, this method of finding the admittance matrix is faster by a factor of ten or more than finite-difference methods. The method is applicable to other problems described by the reduced wave equation.

1. INTRODUCTION

This paper presents an economical method for numerically finding the admittance matrix, at any frequency, of a thin-film distributed resistance-capacitane (DRC) network. The potential in the thin film obeys the partial differential equation

$$\nabla^2\varphi = \gamma^2\varphi, \tag{1}$$

with

$$\gamma^2 = i\omega R_s C \tag{2}$$

in a two-dimensional region, and also obeys linear boundary conditions on the perimeter of the region. Equation (1), the reduced wave equation, describes many important physical phenomena (with different γ^2). It is customarily solved by finite-difference methods, which are very powerful, but which cannot take full advantage of the simplicity of (1), especially in the case to be considered in this paper, when γ^2 is constant over the region in question. In this paper, (1) is reformulated as an integral equation involving the potential and its normal derivative on the perimeter of the network. In this manner, the problem is reduced from a

two-dimensional problem to a one-dimensional one, with attendant savings in computer time.

The integral equation is much more complicated than the differential equation, but an accurate solution for the admittance matrix may be obtained more economically from the integral equation. Results for Laplace's equation and a simple test structure indicate that the present technique finds the conductance in less than one-tenth the time taken by previously published finite-difference method solutions of the same accuracy.

The exposition in this paper will be in terms of the DRC network; extensions for more general problems of type (1) will be considered in Section 5.

2. Formulation

A cross section of a portion of a thin-film DRC network is shown in Fig. 1. When fringing of the electric field in the vertical direction can be ignored, the potential in the resistive layer obeys, in two dimensions,

$$\nabla^2\varphi = \gamma^2\varphi = i\omega R_s C\varphi. \tag{3}$$

φ is the potential difference between the resistive layer and the ground plane; the resistive layer is assumed to be sufficiently thin so that the variation of φ in the direction normal to the ground plane can be ignored.

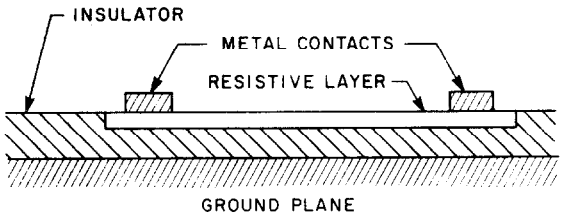

Fig. 1. Cross section of a portion of a thin-film DRC network.

A time dependence of $\exp(i\omega t)$ has been assumed; R_s is the sheet resistance of the resistive layer, and C the capacitance per unit area coupling the resistive layer to the ground plane. Figure 2 shows a top view of a sample DRC network; (3) holds in the resistive layer, the stippled region. The boundary of the resistive region is made up of metal contacts (heavy lines) and of insulating boundaries (light lines). On each of the metal contacts, the boundary condition is that the potential be constant; the current flowing out through the contact is to be found. On each of the insulating

parts of the boundary, the boundary condition is that no current flow out of the resistive region. This is equivalent to the condition that

$$\mathbf{n} \cdot \nabla \varphi = 0 \tag{4}$$

on insulating parts of the boundary; $\mathbf{n}$ is the unit-length outward-pointing normal to the boundary. On insulating parts of the boundary, the potential is to be found. No special difficulty arises with resistive regions which are multiply connected, as in Fig. 2, which has a hole in the resistive layer.

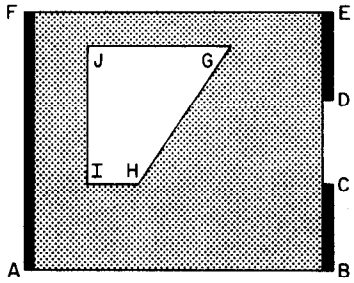

FIG. 2. Top view of a hypothetical DRC network. The dark lines are metal terminals. The resistive layer is surrounded by an insulator, and has a hole in it.

In a way similar to that used by Courant and Hilbert [1] for Laplace's equation, (3) may be reformulated as an integral equation, starting with Green's boundary formula,

$$\iint_D (G\nabla^2\varphi - \varphi\nabla^2 G)\, dx\, dy = \int_\Gamma \left(G \frac{\partial \varphi}{\partial n} - \varphi \frac{\partial G}{\partial n}\right) ds. \tag{5}$$

The area integral is over D, the resistive layer; the line integral is over Γ, the boundary of D. For the example of Fig. 2, D is multiply connected; Γ consists of two parts—an outer rectangle and an inner trapezoid.

The function G will be chosen later to eliminate the area integral. Equation (5) may be rewritten as

$$\iint_D [G(\nabla^2\varphi - \gamma^2\varphi) - \varphi(\nabla^2 G - \gamma^2 G)]\, dx\, dy = \int_\Gamma \left(G \frac{\partial \varphi}{\partial n} - \varphi \frac{\partial G}{\partial n}\right) ds. \tag{6}$$

By virtue of (3), the coefficient of G in the area integrand vanishes. To eliminate the area integral entirely, let G be the Green's function of (3),

$$\begin{aligned} G(x, y; x', y') &= K_0(\gamma r), \\ r^2 &= (x - x')^2 + (y - y')^2, \end{aligned} \tag{7}$$

where (x', y') is any arbitrary point, x and y are the variables of integration in (6), and K_0 is the modified Bessel function of the second kind. Then apply (6) to D', consisting of D minus a small circle of radius ϵ, centered at (x', y'). If (x', y') is on Γ, only the sector of the circle inside D need be excluded. By taking the limit $\epsilon \to 0$, one obtains

$$\sigma(x', y')\, \varphi(x', y') = \int_\Gamma \left[K_0(\gamma r) \frac{\partial \varphi(x, y)}{\partial n} - \varphi(x, y) \frac{\partial K_0(\gamma r)}{\partial n}\right] ds. \tag{8}$$

Here

$$\begin{aligned} \sigma(x', y') &= 2\pi, \quad && \text{for } (x', y') \text{ inside } D, \\ &= \theta, && \text{for } (x', y') \text{ on } \Gamma, \\ &= 0, && \text{for } (x', y') \text{ outside } D; \end{aligned} \tag{9}$$

θ is the interior angle at (x', y') subtended by Γ, equal to π if (x', y') is not a corner point of the boundary. When (x', y') is on the boundary, the integral is to be interpreted as a principal-value integral. For Laplace's equation in two dimensions, (3) with $\gamma = 0$, $K_0(\gamma r)$ must be replaced by $-\ln r$.

From (8) it may be seen that the potential inside the resistive region is determined if the potential and normal gradient are known at each point of the boundary. From the form of (8), it may be verified that the potential inside the resistive region obeys (3) identically. At each point of Γ, either φ or $\partial\varphi/\partial n$ is specified, and the other is to be found. Taking (x', y') on Γ in Eq. (8) results in an integral equation involving only the potential and its normal gradient on the boundary. Thus, the two-dimensional partial differential Eq. (3) has been reduced to a one-dimensional integral equation for φ and $\partial\varphi/\partial n$.

The integral equation may be written as

$$\sigma(s')\, \varphi(s') = P \int_\Gamma [K_0(\gamma r)\, \psi(s) + \gamma(\mathbf{n} \cdot \mathbf{r}/r)\, K_1(\gamma r)\, \varphi(s)]\, ds; \tag{10}$$

the P indicates a Cauchy principle-value integral. Since φ and $\psi \equiv \partial\varphi/\partial n$ are needed only on Γ, the arc length s is used as parameter instead of x and y. The vector $\mathbf{r}$ is from point s' to point s. The Bessel function $K_1(\gamma r)$ arises from [2]

$$\begin{aligned} \frac{\partial}{\partial n} K_0(\gamma r) = \mathbf{n} \cdot \nabla K_0(\gamma r) &= \gamma(\mathbf{n} \cdot \mathbf{r}/r) \frac{\partial}{\partial z} K_0(z)\Big|_{z=\gamma r} \\ &= -\gamma(\mathbf{n} \cdot \mathbf{r}/r)\, K_1(\gamma r). \end{aligned} \tag{11}$$

The geometry involved is shown in Fig. 3; $\mathbf{r}$ and $\mathbf{n}$ are shown for two different s points and one s' point. The integral on the right side of (10) naturally divides into

two parts, since $\psi(s) = 0$ on insulating parts of Γ, and $\varphi(s) =$ constant on each metal contact terminal.

In order to determine the admittance matrix for an M-terminal network, M different solutions are necessary. The k-th solution may conveniently be taken to be that with $\varphi = 1$ on the k-th terminal and $\varphi = 0$ on the remaining terminals. The current through terminal j is then the (j, k) element of the admittance matrix; each solution gives one column of the matrix.

The linear integral equation (10) is of the form

$$a(s)f(s) + P\int b(s, t)f(t)\,dt = c(s), \tag{12}$$

where a, b, and c are known functions, and f is unknown; f is either φ or ψ; $a(s)$ is $-\sigma(s)$ on insulating sides, and zero on metal sides; $c(s)$ comes from the integral over φ on the terminals. When an admittance matrix is desired instead of a single

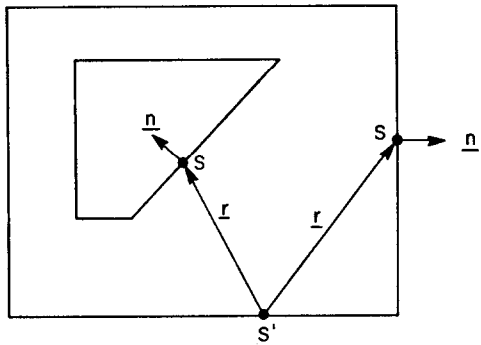

FIG. 3. Geometry of Eq. (10).

solution, (12) is to be solved several times with different right sides but with the same left side. A standard method for the approximate solution of (12) for $f(s)$ is, in principle, quite simple. It consists of two parts. First, $f(s)$ is approximated by a linear combination of N trial functions with undetermined coefficients, say

$$f(s) \simeq g_N(s) \equiv \sum_{k=1}^{N} b_k F_k(s). \tag{13}$$

The usual trial function is a polynomial, particularly one of low order. After (13) is substituted in (12), the integral equation becomes

$$a(s)\sum_{k=1}^{N} b_k F_k(s) + \sum_{k=1}^{N} b_k G_k(s) = c(s), \tag{14}$$

where

$$G_k(s) \equiv P \int F_k(t)\, b(s, t)\, dt. \tag{15}$$

The second part of the solution of (12) is the solution of (14). Because of approximation (13), (14) cannot, in general, be satisfied for every value of u, no matter how the b_k's are chosen. The simplest method is collocation: Choose N values s_j at which to satisfy (14) exactly. Then (14) becomes a set of N linear algebraic equations for the N b_k's, which may be solved by a standard matrix method such as Gaussian elimination. When an admittance matrix is being found, there are N linear equations to be solved, with M different right sides but the same matrix left side. If N is sufficiently large and the s_j are chosen "reasonably", one expects that $g_N(s)$ is a good approximation to $f(s)$, although a formal proof is at best quite difficult. A second method is to choose M values s_j, $M > N$, at which to approximately satisfy (14). Then (14) becomes an overdetermined system of M linear algebraic equations for the N b_k's, and may be solved in the least squares sense or in the Chebyshev sense by a standard library routine.

For the remainder of this paper, only resistive regions bounded by straight-line segments will be considered. This restriction greatly simplifies the geometrical manipulations necessary to deal with otherwise almost arbitrary resistive regions, and allows most of the integrations needed to be done symbolically rather than numerically. With this restriction, (10) may be written

$$\sigma(s')\, \varphi(s') = \sum_m P \int_{\Gamma_m} [K_0(\gamma r)\, \psi_m(s) + \gamma(p/r)\, K_1(\gamma r) \varphi_m(s)]\, ds. \tag{16}$$

The geometry is shown in Fig. 4; the boundary Γ is made up of straight-line segments Γ_m, $m = 1, 2, \ldots, M$. For given s', $\mathbf{n} \cdot \mathbf{r} = p$ is constant on Γ_m. If Γ_m is an insulating side, $\psi_m(s) = 0$ and $\varphi_m(s)$ is to be replaced by a trial function. If Γ_m

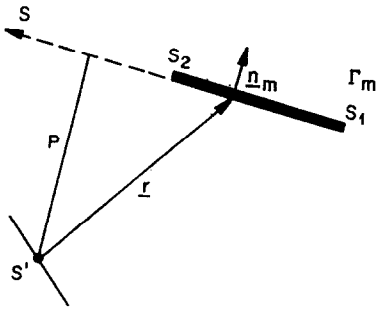

FIG. 4. Geometry of Eq. (16).

is a metallic side, $\varphi_m(s)$ is a constant (either 0 or 1) and $\psi_m(x)$ is to be replaced by a trial function. On each side a different trial function is used. Polynomial trial functions will first be considered; special trial functions will be considered later for use near singular boundary points.

When the trial function for φ_m or ψ_m is a polynomial in s, the integrals in (16) may be done symbolically and then evaluated numerically, rather than being done strictly numerically. This is advantageous because computer time is saved. The symbolic integration may be illustrated by the integral

$$\int_{\Gamma_m} K_0(\gamma r)\,\psi_m(s)\,ds = \int_{s_1}^{s_2} K_0(\gamma r)\Big(\sum b_k s^k\Big)\,ds, \tag{17}$$

where the limits of integration and the trial function for ψ_m have been inserted. From Fig. 4, $r^2 = s^2 + p^2$. Also, $K_0(\gamma r)$ is a function of $\gamma^2 r^2$ only, since [2]

$$K_0(z) = -\Big[E + \frac{1}{2}\ln(z^2/4)\Big]\Big[1 + \frac{z^2/4}{(1!)^2} + \frac{(z^2/4)^2}{(2!)^2} + \cdots\Big] + \frac{z^2/4}{(1!)^2} + \Big(1 + \frac{1}{2}\Big)\frac{(z^2/4)^2}{(2!)^2} + \Big(1 + \frac{1}{2} + \frac{1}{3}\Big)\frac{(z^2/4)^3}{(3!)^2} + \cdots, \tag{18}$$

where E is Euler's constant ($E \approx 0.5772156649...$). Thus the coefficient of b_k in (17) is of the form

$$P\int_{s_1}^{s_2} \{\ln(s^2 + p^2)\cdot Q(s) + R(s)\}\,ds, \tag{19}$$

where Q and R are polynomials in s, and enough terms in the expansion of $K_0(\gamma r)$ are used for the desired accuracy. The polynomials in $r^2 = s^2 + p^2$ are combined symbolically with s^k, the integrals done symbolically, and the limits substituted.

The $K_1\varphi_m$ integral in (16) is done similarly; $(1/\gamma r)\,K_1(\gamma r)$ is a function of $\gamma^2 r^2$ only [2]. The integrals are of the same type as (19) plus another of the type

$$P\int_{s_1}^{s_2} \frac{R(s)}{s^2 + p^2}\,ds. \tag{20}$$

This integral is also done symbolically.

When $|z|$ is large, (18) is not a suitable representation for $K_0(z)$; too many terms are needed for convergence, and too much cancellation takes place, so that accuracy is lost on a finite-precision computer. For large $|z|$, the asymptotic expansion for $K_0(z)$ is used [2],

$$K_0(z) \sim \sqrt{\frac{\pi}{2z}}\,e^{-z}\Big[1 - \frac{1}{8z} + \frac{1\cdot 9}{2!(8z)^2} - \frac{1\cdot 9\cdot 25}{3!(8z)^3} + \cdots\Big]. \tag{21}$$

When this asymptotic expansion and a similar one for $K_1(z)$ are used, then the integrals in (16) must be done numerically. The integrands are quite small, however, since $\mathrm{Re}(\gamma r) > 0$, and are smoothly-varying, so that an automatic Romberg quadrature routine is suitable [3].

For the approximate solution by collocation of (16), a set of points $\{s_j'\}$ must be chosen, one point for each trial function. There is no *a priori* method of choosing the collocation points. However, solving an equation like (14) by collocation is somewhat similar to the problem of approximating a function on $(-1, 1)$ by interpolating a kth-order polynomial to the function at $k + 1$ points in $(-1, 1)$. It is well known [4] that, without having any special knowledge about the function, the maximum error in the approximation is minimized by choosing the interpolation points to be the zeroes of the Chebyshev polynomial of order $k + 1$. Several rules for the allocation of collocation points were considered, all of them such that, if on one side Γ_m, either φ_m or ψ_m, whichever is the unknown, is to be approximated by a kth-order polynomial, $k + 1$ collocation points are chosen on Γ_m. Best results were obtained, as expected, when the $k + 1$ collocation points were chosen as the zeroes of the Chebyshev polynomial of order $k + 1$, shifted from the interval $(-1, 1)$ to the interval (s_1, s_2). Since all the Chebyshev zeroes are inside the interval, all the $\sigma(s')$ in (16) are equal to π.

Singular Boundary Points

"Singular corners" in the boundary force correspondingly singular behavior in the potential near the corners. For this purpose, a corner is defined as singular if a metallic side and an insulating side meet at a corner whose interior angle is not $\pi/2$, or if two metallic sides or two insulating sides meet at an angle other than π. (Exceptions to the definition will be noted later.) A singular corner of the first type is shown in Fig. 5, together with polar coordinates (ρ, θ) centered at the corner. Near such a corner, the potential does not have a convergent two-dimensional Taylor series expansion about the singular corner; a low-order polynomial is a poor approximation to the potential or normal gradient. Instead, the potential near the corner may be expanded as

$$\varphi(\rho, \theta) = \varphi_0 + \sum_n f_{\nu_n}(\rho)[A_n \sin \nu_n\theta + B_n \cos \nu_n\theta]. \tag{22}$$

For (3), $f_\nu(\rho) = I_\nu(\gamma\rho)$, the modified Bessel function of the first kind [2]. For Laplace's equation, $f_\nu(\rho) = \rho^\nu$. The ν's depend upon the geometry of the corner, and are chosen to meet the boundary conditions, and the A's and B's depend on conditions away from the corner. For the example of Fig. 5, to satisfy the boundary

conditions of $\varphi =$ constant on $\theta = 0$ and $\psi = (1/\rho)\,\partial\varphi/\partial\theta = 0$ at $\theta = \theta_c$, the cosine terms must vanish and

$$\nu_n = (2n - 1)\,\pi/2\theta_c\,, \tag{23}$$

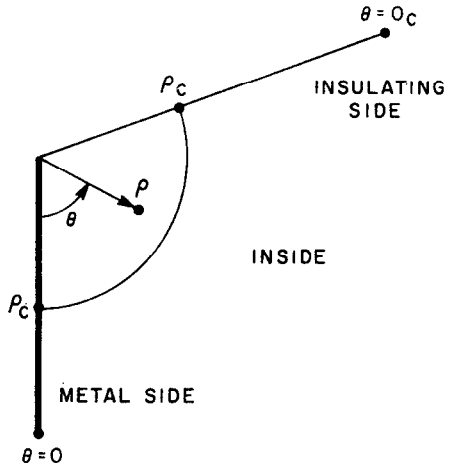

FIG. 5. Geometry at singular corner.

so that

$$\varphi(\rho, \theta) = \varphi_0 + A_1 I_{\pi/2\theta_c}(\gamma\rho) \sin \frac{\pi\theta}{2\theta_c} + A_2 I_{3\pi/2\theta_c}(\gamma\rho) \sin \frac{3\pi\theta}{2\theta_c} + \cdots . \tag{24}$$

On the insulating side, $\theta = \theta_c$,

$$\varphi(\rho, \theta_c) = \varphi_0 + A_1 I_{\pi/2\theta_c}(\gamma\rho) - A_2 I_{3\pi/2\theta_c}(\gamma\rho) + \cdots . \tag{25}$$

Since for small $| z |$, $I_\nu(z) \sim z^\nu$, the first two terms are expected to be most important near the corner, unless A_1 fortuitously is very much smaller than A_2. For large $| z |$ (see Ref. [2]),

$$I_\nu(z) \sim \frac{e^z}{\sqrt{2\pi z}} \left\{1 - \frac{4\nu^2 - 1}{8z} + \cdots\right\}, \tag{26}$$

so that, in general, all the terms are needed and there is large cancellation in (25). For improving the approximate potential, only the small ρ behavior is important, so the trial function used near the singular corner is

$$\varphi(\rho, \theta_c) = \varphi_0 + A_1 \rho^{\pi/2\theta_c}, \tag{27}$$

instead of a polynomial. Similarly, on $\theta = 0$,

$$\psi(\rho, 0) = -\frac{1}{\rho} \frac{\partial \varphi(\rho, \theta)}{\partial \theta}\Big|_{\theta=0}, \tag{28}$$

$$\psi(\rho, 0) = -A_1 \frac{\pi}{2\theta_c \rho} I_{\pi/2\theta_c}(\gamma\rho) - A_2 \frac{3\pi}{2\theta_c \rho} I_{3\pi/2\theta_c}(\gamma\rho) - \cdots . \tag{29}$$

The trial function used near the singular corner is

$$\psi(\rho, 0) = -A_1 \frac{\pi}{2\theta_c} \rho^{((\pi/2\theta_c)-1)}, \tag{30}$$

instead of a polynomial.

Similarly, for two metallic sides or two insulating sides meeting at a corner with interior angle θ_c, $\nu_n = n\pi/\theta_c$. In (22), only the sine terms are present for the metallic corner, and only the cosine terms for the insulating corners. The trial function used at a metallic corner is

$$\psi(\rho, 0) = \psi(\rho, \theta_c) = A_1 \frac{\pi}{\theta_c} \rho^{((\pi/\theta_c)-1)}, \tag{31}$$

and that used at an insulating corner is

$$\begin{aligned} \varphi(\rho, 0) &= \varphi_0 + B_1 \rho^{\pi/\theta_c}, \\ \varphi(\rho, \theta_c) &= \varphi_0 - B_1 \rho^{\pi/\theta_c}. \end{aligned} \tag{32}$$

For some angles θ_c, the ν's turn out to be integers. A frequently occurring example is two metallic (or insulating) sides meeting with interior angle of $\pi/2$. For such corners, the Taylor series does converge, but has some terms missing; these corners need not be treated as singular.

On the two sides adjacent to a singular corner, for ρ less than some ρ_c, the above trial functions are used; for ρ larger than ρ_c, polynomial trial functions are used. There is no *a priori* method of choosing ρ_c, although qualitative arguments may be made. If ρ_c is chosen too large, these trial functions will be inadequate since φ does not behave like ρ^ν far from the corner. If ρ_c is chosen too small, these trial functions will be adequate near the corner, but for $\rho > \rho_c$ the potential still behaves like ρ^ν and the polynomial trial functions will be inadequate. One criterion for choosing ρ_c is based upon the lengths of the two sides adjacent to the corner. Along an adjacent side one expects the potential to vary like ρ^ν and then to vary smoothly; if the next corner is singular, the potential will have another ρ^ν behavior about that corner. A $\rho_{\max}$ may somewhat arbitrarily be defined as one-half the side length if the next corner is regular, and one-third the side length if the next corner

is singular; if the two sides adjacent to a singular corner result in different values for $\rho_{\max}$ calculated in this way, the smaller value is taken. The numerical calculations done assume ρ_c to be $\alpha\rho_{\max}$, with $\rho_{\max}$ calculated in this way; numerical experiments are necessary to determine useful values of the parameter α.

At a singular corner where at least one of the two adjacent sides is a metal, one new trial function is introduced and one new collocation point is used, φ_0 being given as part of the boundary conditions. The extra collocation point is placed exactly on the singular corner; $\sigma(s')$ in (16) is then equal to θ_c.

At a singular corner where both adjacent sides are insulating, two new trial functions are introduced and two new collocation points are used, φ_0 and B_1 both being unknown. The two extra collocation points are placed at $\rho = \rho_c/2$, $\theta = 0$ and $\theta = \theta_c$; $\sigma(s')$ in (16) is then equal to π.

The integrals in (16) now include some over singular corners; these must be done numerically, unless $\rho = \mathbf{n} \cdot \mathbf{r}$ is zero, in which case they can be done symbolically. The necessary integrals are of the type

$$\int_0^{\rho_c} \rho^\nu G(\rho)\, d\rho, \tag{33}$$

with $\nu > -1$, and $G(\rho)$ a smooth function. A special method was devised for these integrals [5].

4. Comparison of Finite-Difference Methods and Boundary Integral Equation Method

Finite-difference techniques have frequently been used to solve partial differential equations like (3). They have the great advantage of being easy to program for computer solution, but have other, well-known, disadvantages. Finite-difference methods start by superposing a two-dimensional grid, usually rectangular, on the area in question. The potential is found only at the vertices of the grid. If the boundary does not coincide with the grid lines, more complicated programming is necessary. The Laplacian operator is approximated by a difference operator at each vertex, and (3) is replaced by a number of linear algebraic equations, one for each vertex. In virtually all cases of practical interest, there are too many equations to be solved directly (for instance by Gaussian elimination) and the equations are solved iteratively. Again, the iteration converges well for simple, compact areas, using successive overrelaxation or similar methods, but for complicated boundaries the iteration is not guaranteed and, in general, a reasonably efficient scheme is not known and must be determined. At the conclusion of the iteration, an approximation to the potential is known at each vertex point. The

normal derivative at the metal boundaries, ψ, is found by numerical differentiation, and is integrated to obtain the admittance. If the admittance matrix of a multiterminal structure is desired, this process must be done once for each terminal. Since the iteration takes most of the solution time, no savings in time is available.

The boundary integral equation technique overcomes these disadvantages at the cost of more complicated computer programming. No grid is necessary, and nonorthogonal boundary lines cause no special difficulty. The integral equation is approximated by a set of linear algebraic equations, and there are, in general, few enough equations to be solved by Gaussian elimination. Solving the linear equations takes only a small part of the total computing time, and no iteration is necessary. After the linear equations have been solved, an approximation to the potential and to its normal derivative is known, on all boundaries of the figure, in functional form rather than at isolated points. No numerical differentiation is necessary—the admittance is obtained by a straightforward integration of the normal derivative. If the admittance matrix of a multiterminal structure is desired, the problem is reduced to setting up and solving a set of linear algebraic equations with a number of different right sides, and takes very little more computing time than if only one column of the admittance matrix is desired.

It is not necessary to find the potential inside the figure in order to obtain the admittance, but the potential may be obtained by doing an integral, (16) with $\sigma = 2\pi$ and s' inside the resistive region, which is virtually identical to the integrals done in setting up the set of linear algebraic equations. The potential in the interior automatically satisfies the differential equation, by construction. Finally, the boundary integral equation technique is significantly faster than even sophisticated finite difference methods.

Integral equation formulations of the Helmholtz equation for acoustic radiation from a three-dimensional surface have been used for some time [6]. Apparently, Jaswon and Symm [7, 8] were the first to use similar integral equation formulations for Laplace's equation in electrostatics. Arnold [9] also used Green's boundary-value formula for solving Laplace's equation. Chawla and Gummel [10] used an integral equation formulation based on the Cauchy integral formula to solve Laplace's equation.

5. Extensions

Equation (1) may be solved by the method described earlier, with any linear boundary condition of the form

$$F(s)\,\varphi(s) + G(s)\,\psi(s) = H(s), \tag{34}$$

where F, G, and H are given functions on the boundary of the region inside which (1) is to be solved.

The inhomogeneous form of (1),

$$\nabla^2\varphi - \gamma^2\varphi = f(x, y), \tag{35}$$

where f is a given function, may be solved by the method described earlier. One way is to find a function $F(x, y)$ which obeys (35) but not the boundary conditions, and then use the method described in this paper on the difference $\varphi - F$ with new boundary conditions. When $f(x, y)$ is a polynomial in x and y, F is easily found; then the integrals of (16) may be done symbolically as before, since F is a polynomial in s on each side Γ_m. If such a function F cannot be found, a different integral equation may be obtained by substituting (35) into (6); then an area integral,

$$-\iint_D K_0(\gamma r) f(x, y)\, dx\, dy, \tag{36}$$

must be added to the right side of (10).

If γ^2 is a function of x and y instead of a constant, the method is not applicable unless a Green's function can be found; in this case G will not be a function of r only, but of x, y, x', y'. If, however, γ^2 takes on different constant values over subregions, (10) may be applied in each subregion, with both φ and ψ regarded as unknowns. Additional boundary conditions will be necessary on the boundaries of the subregion; these will depend on the physical problem being modeled. Such a case has been treated by Blue [13].

6. Numerical Results

Computer programs were written to solve for the admittance matrix of a thin-film DRC network bounded by straight-line segments. The thin film may be multiply connected, and need not be restricted to any particular number of metal terminals or insulating sides. Any value of $\omega R_s C$ may be specified. Similar programs were written to solve Laplace's equation for the dc conductance matrix of a distributed thin-film resistive network. Because complex arithmetic need not be used, and because the Green's function $\ln(1/r)$ is simpler to work with than $K_0(\gamma r)$, this version runs considerably faster than the complex version.

The programs were designed to give accuracies in the range of 10 %–0.01 % for admittance matrix elements. In this range, the collocation method is suitable; if considerably more accuracy is desired, a least square or Chebyshev solution of an overdetermined set of equations would be necessary. The computer time used is approximately proportional to the product of N, the number of trial functions, and M, the number of points at which (14) is evaluated ($M = N$ for the collocation

method). The time used to solve the linear equations is insignificant compared to the time needed to set up the equations for N and M of the order of 50 or less.

The computer programs were designed to be used as part of a large package which analyzes integrated circuits, and so must work automatically, with no hand-tailoring for particular networks. The programs allocate the collocation points and decide, based on comparison of successive analyses, if the requested accuracy has been attained, or if it cannot be attained within the allowed bounds on computer time and memory. Studies were made of the convergence of the admittance matrix as a function of the number of trial functions and of the algorithm for placing the collocation points. These studies were made almost exclusively on Laplace's equation, since conformal transformations and symmetry considerations allow conductance matrices to be calculated for an unlimited number of two-terminal networks. Some of the networks analyzed are shown in Fig. 6, together with their conductances g; the conductance matrices are of the form

$$\begin{pmatrix} g & -g \\ -g & g \end{pmatrix}.$$

The first set of tests was designed to check the placing of collocation points. Three algorithms were considered for placing k points on a side: the zeroes of the Chebyshev polynomial T_k, shifted from $(-1, 1)$ to (s_1, s_2); the zeroes of the Legendre polynomial P_k, similarly shifted; and points equally spaced on the side, at $s_1 + h/2, s_1 + 3h/2, \ldots, s_2 - h/2$, where $h = (s_2 - s_1)/k$. On each side, the unknown φ or ψ was approximated by a polynomial trial function; the same order polynomial was used on each side.

Each calculation yields an approximate conductance matrix of the form

$$\begin{pmatrix} g_1 & -g_2 \\ -g_2 & g_1 \end{pmatrix};$$

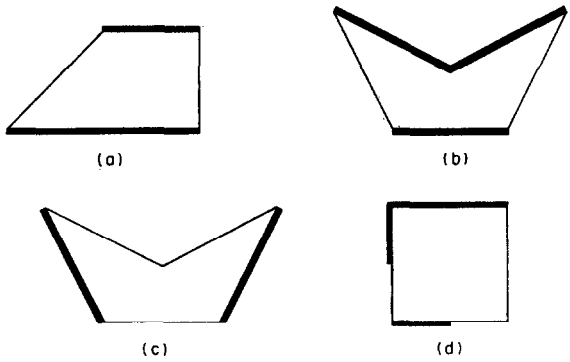

FIG. 6. Test networks. Conductances g are: (a) 1.2792616, (b) 2.0, (c) 0.5, (d) 1.0.

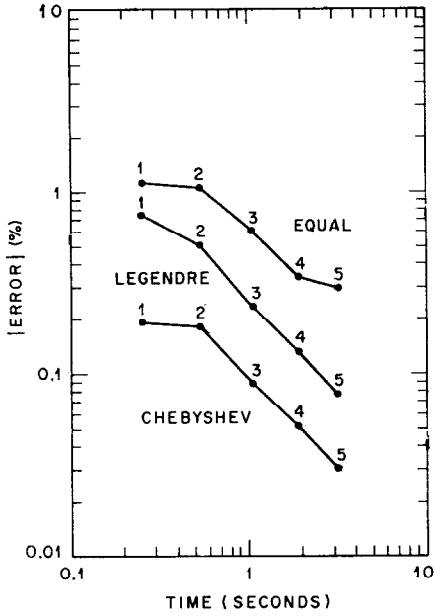

FIG. 7. Accuracy vs time plot for Fig. 6a, for three collocation methods, for polynomial trial functions of orders one through five.

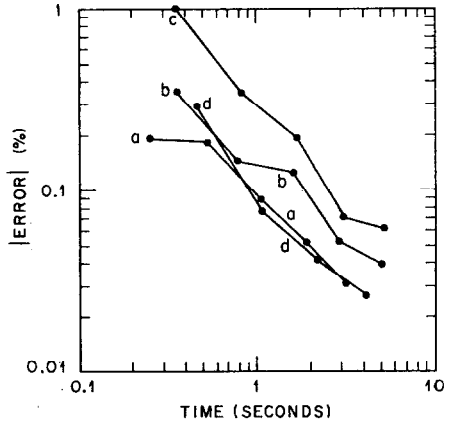

FIG. 8. Accuracy vs time plot for Fig. 6a–6d, Chebyshev collocation, polynomials of orders one through five.

in general, g_1 and g_2 are not equal. Figure 7 contains a plot of the larger of the conductance errors $|g_{true} - g_1|$ and $|g_{true} - g_2|$ vs. the computer time used (GE 635) for three collocation algorithms and the structure of Fig. 6a. The numbers are the orders of the polynomial trial functions used. As expected using the Chebyshev zeroes gives a better result than the other two methods. This was also found to be true for the other networks of Fig. 6. Their accuracy vs. time plots are very similar to Fig. 7, with "Chebyshev" below "Legendre" by a factor of two or three, and below "equal" by a factor of ten. For comparison, Fig. 8 has accuracy vs. time plots of the four networks, using Chebyshev zeroes as collocation points.

If an improved admittance matrix is desired and polynomial trial functions are being used, one could use higher order polynomials on each side, or subdivide the sides and use the same order of polynomials. For Laplace's equation, and for (3) with $\omega R_s C$ not too high, the former procedure proved to be better, up to a point.

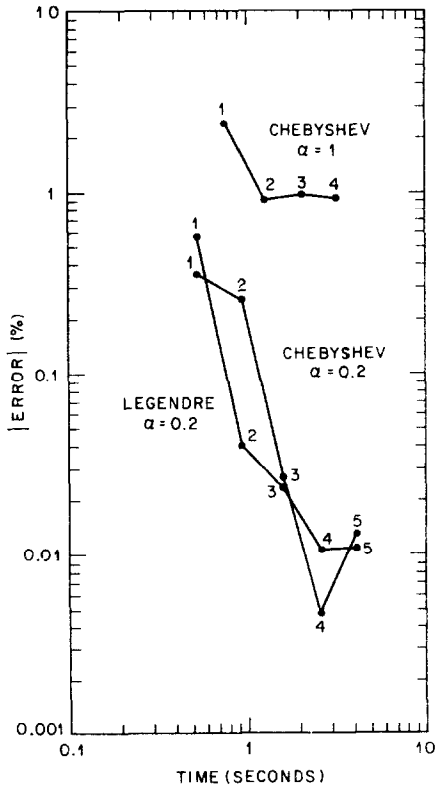

FIG. 9. Accuracy vs. time plot for Fig. 6a, $\alpha = 1$ and $\alpha = 0.2$, Chebyshev collocation, polynomials of indicated orders.

If the order is too high, the matrix of the linear equations becomes ill-conditioned, and accuracy is lost. For the GE 635, with approximately 8-digit words, this point was reached for sixth or eighth order polynomials. If $\omega R_s C$ is very high, the potential on some sides is a rapidly-decaying complex exponential function, which cannot be well approximated by a low-order polynomial unless the side is subdivided. (For the proposed application, this circumstance is not expected to occur frequently.)

Some tests were also made using nonpolynomial trial functions at singular corners. For the network of Fig. 6a, accuracy vs. time plots are shown in Fig. 9, for $\alpha = \rho_c/\rho_{\max}$ of 1 and 0.2; Chebyshev zero collocation points were used on the sides away from the singular corners. For $\alpha = 1$, the conductance is limited in accuracy to about 1% because ρ_c is too large. For $\alpha = 1/5$, the conductance is limited in accuracy to about 0.01% because the integrals (33) are done to an accuracy of 10^{-6}. For $\alpha = 1$, the error is much worse, and for $\alpha = 1/5$ much better, than the error if only polynomial trial functions are used. Similar results are obtained with the other collocation methods; Chebyshev is only slightly better than Legendre, which is slightly better than equal. In general, α in the range of 1/5–1/10 was best; α too large is much worse than α too small. An all-purpose algorithm is difficult to prescribe; perhaps the best is to choose α small, 1/5 or

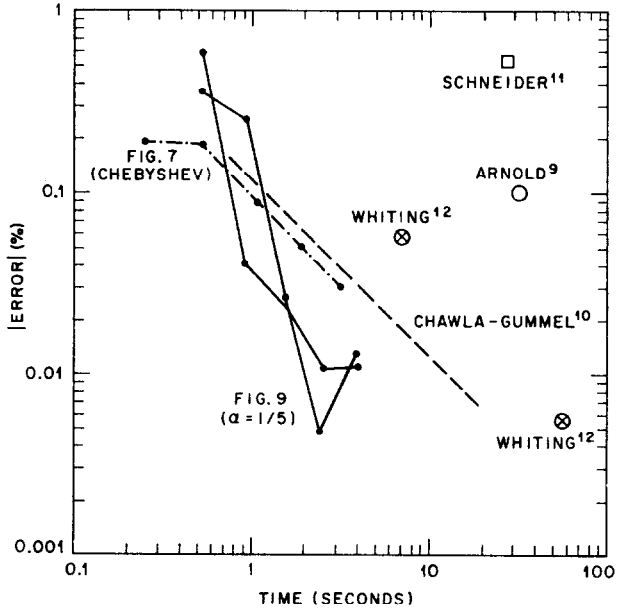

FIG. 10. Accuracy vs. time plot for Fig. 6a, various authors. After Chawla and Gummel [10].

1/10 or less, and to use polynomials of order four or less. Additional trial functions in the series (22) could also be used; this was not tested numerically. For comparison, Fig. 10 has results from Figs. 7 and 9, together with results from other calculations on the same network. The errors plotted for the other authors are presumably those for the mean conductance $(g_1 + g_2)/2$; they are taken from Chawla and Gummel [10]. Schneider [11] and Whiting [12] did not solve for the conductance of a network, but solved the isomorphic problem of finding the capacitance of a coaxial transmission line. Corrections were made by Chawla and Gummel to allow for the different computer, the IBM 7094, used by Schneider and by Whiting.

Note Added

The author wishes to thank the referee for calling his attention to the work of E. G. Cristal [14], who compared finite-difference methods with the integral equation method for coupled round rods between ground planes.

References

1. R. Courant and D. Hilbert, "Methods of Mathematical Physics," Vol. II, pp. 252–6, Interscience, New York, 1962.
2. M. Abramowitz and I. Stegun, Eds., "Handbook of Mathematical Functions," pp. 374–379, National Bureau of Standards, Washington, D. C., 1964.
3. A. Ralston, "A First Course in Numerical Analysis," p. 121, McGraw-Hill, New York, 1965.
4. R. W. Hamming, "Numerical Methods for Scientists and Engineers," p. 253, McGraw-Hill, New York, 1962.
5. J. L. Blue, "Adaptive Simpson quadrature with weight function X^{ν}," unpublished.
6. F. H. Fenlon, Calculation of the acoustic radiation field at the surface of a finite cylinder by the method of weighted residuals, *Proc. IEEE*, **57** (1969), 291–306 and references therein.
7. M. A. Jaswon, Integral equation methods in potential theory I, *Proc. Roy. Soc.* **A275** (1963), 23–32.
8. G. T. Symm, *Proc. Roy. Soc.* **A275** (1963), 33.
9. S. R. Arnold, Two-dimensional conductance calculation employing Green's boundary value formula, in "Computer-Aided Integrated Circuits and Device Design" (R. B. Schilling, Ed.), McGraw-Hill, New York, to be published.
10. B. R. Chawla and H. K. Gummel, A boundary technique for calculation of distributed resistance, *IEEE Trans. Electron Devices* **17** (1970), 915–925.
11. M. V. Schneider, Computation of impedance and attentuation of TEM-lines by finite difference methods, *IEEE Trans. Microwave Theory Techniques*, **13** (1965), 793–800.
12. K. B. Whiting, A treatment for boundary singularities in finite difference solutions of Laplace's equation, *IEEE Trans. Microwave Theory Techniques*, **13** (1968), 889–891.

13. J. L. BLUE, "Two-Dimensional Distributed Base-Resistance Effects in Bipolar Transistors," talk presented at International Electron Devices Meeting, Washington, D. C., October 31, 1969.
14. E. G. CRISTAL, "A Comparison of Two Computer Methods for Solving TEM Problems," talk WAM-II-6, presented at 1969 International Microwave Symposium, Dallas, Texas, May 7, 1969.